Measurement of cross-sections in some reactions in $^{16}O+^{181}Ta$ system at energies ~5 MeV/nucleon

R. Prasad[1], Devendra P. Singh[1], Abhishek Yadav[1], Pushpendra P. Singh[1], Unnati[1], Manoj Kumar Sharma[1], B. P. Singh[1], Rakesh Kumar[2] and K. S. Golda[2]

[1]Department of Physics, Aligarh Muslim University, Aligarh (UP)-202 002, INDIA
[2]Inter-University Accelerator Center, New Delhi -110 067, INDIA

Email contact of main author: rpm166@rediffmail.com

Abstract. An experiment has been carried out to explore heavy ion in-complete fusion reaction dynamics within the framework of break-up fusion model at energies near and above the Coulomb barrier. Excitation functions for several radio-nuclides produced via xn, pxn and αxn-channels have been measured in $^{16}O + ^{181}Ta$ system at energies ≈ 76-100 MeV. The experimental excitation functions have been compared with those calculated using theoretical model code PACE4. It has been observed that, excitation functions of xn/pxn-channels are in good agreement with theoretical predictions. However, a significant enhancement in the measured excitation functions of α-emitting channels have been observed, which may be attributed to the in-complete fusion processes. The in-complete fusion fraction (FICF) which gives the relative importance of complete and in-complete fusion processes has been found to increase with energy.

1. Introduction

For many years, the study of heavy ion (HI) induced reactions has been used as an important tool to understand the reaction dynamics and the decay characteristics of excited compound nucleus (CN) at energies near and above the Coulomb barrier (CB)[1-2]. It is now experimentally established that complete (CF) and incomplete fusion (ICF) are the most dominating modes of reaction processes at these energies [3-6]. In case of CF, all the nucleons of projectile and target nucleus lose their identity and form a single, excited complex system, which may eventually lead to a fully equilibrated CN. The equilibrium state occurs, as the composite system produces an intense mean field that prevents the escaping of nucleons from the excited complex system and leads to complete thermalization. At later stages, the CN de-excites via emission of light nuclear particle(s) and/or the characteristic γ-rays. However, in case of ICF, as the projectile comes within the field of target nucleus, it is assumed to break-up into its fragments (predominantly into α-clusters, in case of the projectiles having α-cluster structure), where one of the fragments may get fused with the target nucleus leading to the formation of an excited incompletely fused composite (IFC) system with a mass and/or charge less than the CN formed via CF. The un-fused fragment flows in forward cone with almost projectile velocity. Further, it has also been observed that, apart from CF and ICF, pre-equilibrium (PE) emission of light nuclear particles may also take place at these energies before the thermalization of composite system [7]. Recently, it has been observed that ICF becomes more and more dominant as the projectile energy increases [8-10]. The different modes of reactions can also be understood on the basis of driving input angular momenta imparted into the system. The CF occurs for the input angular momenta values $\leq l_{crit}$, as per the sharp cut-off approximation. However, at relatively higher projectile energies and/or at larger impact parameters, ICF start influencing the CF. It may, further, be pointed out that the multitude of driving input angular momenta may vary with the projectile energy and/or with the impact parameter. However, there is no sharp boundary for the CF and ICF processes, both the processes have been observed below and/or above the limiting

value of input angular momenta. A few reports have indicated that ICF can selectively populate high spin states in the final reaction products at low bombarding energies and can be used as a spectroscopic tool as well[11]. The ICF reactions have been demonstrated to populate neutron rich nuclei compared to conventional fusion-evaporation reactions opening possibilities for the study of nuclei along the neutron rich side of the line of stability [12].

A variety of dynamical models/theories, like; Breakup Fusion (BUF) model[13], SUMRULE model [14], Promptly Emitted Particles (PEPs) model[15], EXCITON model[16], the Hot Spot model [17], the Multi-step Direct Reaction Theory [18] and Overlap model [19] have been proposed to explain ICF dynamics. Apart from the aforementioned dynamical models, Morgenstern et. al. [20], investigated mass-asymmetry dependence of ICF contribution. The details of the above models are given in ref.[9]. It may, however, be pointed out that these models correctly predict the magnitude of ICF, to some extent, in some cases at energies $\geq$ 10 MeV/nucleon, but none of these models/theories is able to successfully explain the ICF data at energies ≈4-7 MeV/nucleon. As such, the study of ICF is still an active area of investigation. Despite the existence of so many models, a clear picture of the mechanism of ICF is yet to emerge particularly at relatively low bombarding energies i.e.≈4-7 MeV/nucleon, where the systematic study is available only for a few projectile target combinations [3,9].

As such, for better understanding of ICF dynamics at low energies, excitation functions (EFs) for several radionuclide produced in the $^{16}O+^{181}Ta$ system ($Z_1.Z_2$=584), have been measured in the projectile energy range ≈76 -100 MeV. In the present work, cross-sections have been measured for those residues which may be populated via ICF processes as well. Further, in the present work, an attempt has also been made to estimate the relative contribution of CF and ICF in order to study the influence of ICF on CF processes.

2. Experimental procedure

In the present work, experiment has been performed using $^{16}O^{7+}$ beam delivered from 15UD-Pelletron Accelerator at the Inter University Accelerator Centre (IUAC), New Delhi, India. Targets of spectroscopically pure ^{181}Ta (≈ 99.99 %) of thickness ≈ 1.5 mg/cm^2 were prepared by rolling technique. In order to trap the recoiling products produced via different reaction processes, Al-catchers of appropriate thickness were placed after each target. The thickness of each target and catcher foil were separately measured by weighing, and also by α-transmission method. Irradiations have been carried out in the General Purpose Scattering Chamber (GPSC), having an in-vacuum transfer facility (ITF). The targets along with Al-catchers in the form of a stack were placed normal to the beam direction, so that the recoiling products may be trapped in the catcher foils. The experimental set-up is similar to that given in ref.[9]. Keeping in view the half-lives of interest, irradiations have been carried out for ≈8-10 hrs for each stack. The activities produced after irradiation were recorded using a pre-calibrated, High Purity Germanium (HPGe) detector of 100 c.c. active volume coupled to a PC through CAMAC based FREEDOM software. The efficiency of the detector has been determined at various source-detector separations. Confirmation of the identification of reaction products have been made by the decay curve analysis and also by the characteristic γ-rays. Identified residues along with their important spectroscopic properties are given in Table I. The experimentally measured cross-sections for the population of residues via CF and/or ICF processes are given in Tables 2-3. The

overall errors in the present work are estimated to be ≤15 %, including the statistical errors. Details of errors are given in ref.[9].

TABLE 1: LIST OF REACTION PRODUCTS ALONG WITH POPULATED CHANNELS AND THEIR SPECTROSCOPIC PROPERTIES.

Residue T	$_{1/2}$	J^{π}	E_{γ} **(keV)**	I_{γ}**(%)**
^{194m}Tl(3n)	32.8 min	7^{+}	636.1	99
^{194g}Tl(3n)	33 min	2^{-}	636.1	15.3
^{193g}Tl(4n)	21.6 min	$1/2^{+}$	324.4,1044.7	15.2, 8.99
^{192m}Tl(5n)	10.6 min	7^{+}	422.9	31.1
^{192g}Tl(5n)	9.6 min	2^{-}	422.9	31.1
^{193g}Hg(p3n)	3.8hrs	$3/2^{-}$	381.6, 861.1	11.0, 13.0
^{193m}Hg(p3n)	11.8 hrs	$3/2^{-}$	258.1	60.0
^{192}Hg(p4n)	4.85 hrs	0^{+}	274.8	50.4
^{191g}Hg(p5n)	49 min	$3/2^{-}$	224.6, 331.7	17.4, 11.24
^{191m}Hg(p5n)	50.8 min	$13/2^{+}$	420.3,578.7	17.9,17.0
^{192g}Au(αn)	4.94 hrs	1^{-}	295.5, 316.5	22.7, 58.0
^{191g}Au(α2n)	3.18 hrs	$3/2^{+}$	283.9, 399.8	6.3, 4.5
^{190g}Au(α3n)	42.8 min	1^{-}	295.9, 301.9	71.0, 25.1

TABLE 2: EXPERIMENTALLY MEASURED CROSS-SECTIONS FOR THE RESIDUES POPULATED IN THE INTERACTION OF ^{16}O WITH ^{181}Ta SYSTEM. THE VALUES OF CROSS-SECTIONS ARE IN MB.

E_{Lab} **(MeV)**	^{194m}**Tl**	^{194g}**Tl**	^{193g}**Tl**	^{192m}**Tl**	^{192g}**Tl**	^{193g}**Hg**
76 ±1.1	2±0.2	2±0.2	26±3.8	-	-	23±3.5
80 ± 1.5	6±0.8	6±0.8	45±6.8	22±3.2	22±3.2	47±7.0
85 ± 1.2	4±0.5	4±0.5	68±10.2	61±9.1	61±9.1	60±8.9
87 ± 1.0	3±0.4	3±0.4	46±6.9	44±6.5	44±6.5	49±7.4
88 ± 1.6	2±0.2	2±0.2	44±6.5	91±13.7	91±13.7	42±6.2
93 ± 1.1	2.5±0.3	2±0.3	35±5.2	184±27.6	184±27.6	29±4.4
97 ± 1.0	2±0.3	1.5±0.2	15±2.3	171±25.5	171±25.5	12±1.7
99 ± 0.9	1±0.1	1±0.1	17±2.5	222±33.3	222±33.3	10±1.5

3. Results and analysis of data

In order to study the ICF reaction dynamics in ^{16}O+ ^{181}Ta system, the EFs for ^{194g}Tl, ^{194m}Tl, ^{193g}Tl, ^{192g}Tl, ^{192m}Tl, ^{192m}Tl, ^{193g}Hg, ^{193m}Hg, ^{192}Hg, ^{191g}Hg, ^{191m}Hg, ^{192g}Au, ^{191g}Au, and ^{190g}Au radio nuclides expected to be populated via CF and/or ICF have been measured. In general, a residue populated via a specific channel often emits several γ-rays of different energies. The cross-section for the channel has been determined from the measured intensities of several characteristic γ-rays and the value quoted is the weighted average of cross-sections obtained for these γ-rays. The measured EFs for residues populated via xn-channels are shown in Fig.2(a). From the analysis of experimental data, activities corresponding to 3n, 4n & 5n channels have been identified. It may be pointed out that in case of 3n and 5n channels meta-stable and ground states of ^{194}Tl and ^{192}Tl are plotted. In both these cases, the meta-stable and ground states of the

respective residues decay with γ-rays of nearly same energy and half-lives. As such, the observed composite decay curves gave the sum of both the states in each case. Individual cross-sections have been obtained by dividing the measured composite cross-sections in the ratio of their γ-ray intensities [21,22]. The ^{193g,m}Tl are populated by 4n channel. The meta-stable state of half-life ≈ 2 min., decays to the ground state which has a half-life of ≈22 min. Since, counting of the irradiated samples was done after about 10 min. from the stop of irradiation, the measured cross-sections for the ground state also contain contribution (≤0.38 %) of the meta-stable state.

TABLE 3: EXPERIMENTALLY MEASURED CROSS-SECTIONS FOR THE RESIDUES POPULATED IN THE INTERACTION OF ^{16}O WITH ^{181}Ta SYSTEM. THE VALUES OF CROSS-SECTIONS ARE IN MB.

E_{Lab} (MeV)	**^{193m}Hg**	**^{192}Hg**	**^{191g}Hg**	**^{191m}Hg**	**^{192g}Au**	**^{191g}Au**	**^{190g}Au**
76 ±1.1	8±0.8						
80 ± 1.5	21±2.1	4±0.5	-	-	2±0.2	-	-
85 ± 1.2	30±3.0	40±6.0	-	-	10±1.5	-	8±1.3
87 ± 1.0	22±2.2	36±5.5	-	-	12±1.8	2±0.3	6±0.8
88 ± 1.6	24±2.3	65± 9.8	3±0.5	0.3±0.04	31±4.6	2±0.3	23±3.5
93 ± 1.1	13±1.3	121±18.2	5±0.7	3±0.5	46±6.9	3±0.5	20±2.9
97 ± 1.0	8 ±0.7	131 ±6	7±.9	8±1.2	63±9.5	14±2.1	40±5.9
99 ± 0.9	6±0.5	154 ±23.2	14±2.1	18±2.7	50±7.5	22±3.2	21±3.2

The sum of cross-sections ($\Sigma\sigma_{xn}$) for all the populated residues produced via xn(x=3, 4 & 5) channels is shown in Fig.2(a), indicating the initial rise in $\Sigma\sigma_{xn}$ values and then nearly saturating at higher energies. In case of pxn channels, residues corresponding to p3n, p4n & p5n channels have been identified through their characteristic γ-rays and also by the respective half-lives. All the residues in pxn cases, decay independently with their respective half-lives and γ-rays of known energies. The cross-sections for these channels are plotted in Fig. 2(b) and are tabulated in Tables 2 & 3. In Fig.2(b), the sum of cross-sections for all measured pxn channels, denoted by $\Sigma\sigma_{pxn}$ has been obtained by adding the measured cross-sections for p3n, p4n and p5n channels. In order to determine the total measured fusion cross-section $\Sigma\sigma_{CF}$ (expt), the sum of cross-sections due to xn channels i.e., $\Sigma\sigma_{xn}$ and the sum of cross-sections due to all measured pxn channels i.e., $\Sigma\sigma_{pxn}$ have been added. The total $\Sigma\sigma_{CF}$ (expt) shown in Fig.2(c) has been compared with $\Sigma\sigma_{CF}$ (Theoretical) obtained using code PACE4[23] with different values of level density parameters a(=A/K). As can be seen from Fig.2(c), the $\Sigma\sigma_{CF}$ (expt) is in good agreement with theoretical $\Sigma\sigma_{CF}$ values. The fact that the measured fusion cross-section $\Sigma\sigma_{CF}$ (expt) could be reproduced satisfactorily by PACE4 predictions, strengthens the confidence to the choice of input parameters. In Fig.2(d), the measured cross-sections for the population of $^{193-x}$Au (x= 1, 2 & 3) isotopes via αxn channels are shown. It may be mentioned that in case of αxn channels, the residue may be formed in two ways; (i) by CF of ^{16}O followed by the formation of an excited CN from which evaporation of neutrons and α-particles takes place, (ii) on the other hand, if it is assumed that the ^{16}O ion breaks into α + ^{12}C and ^{12}C fuses with the target leaving α particle as an spectator.

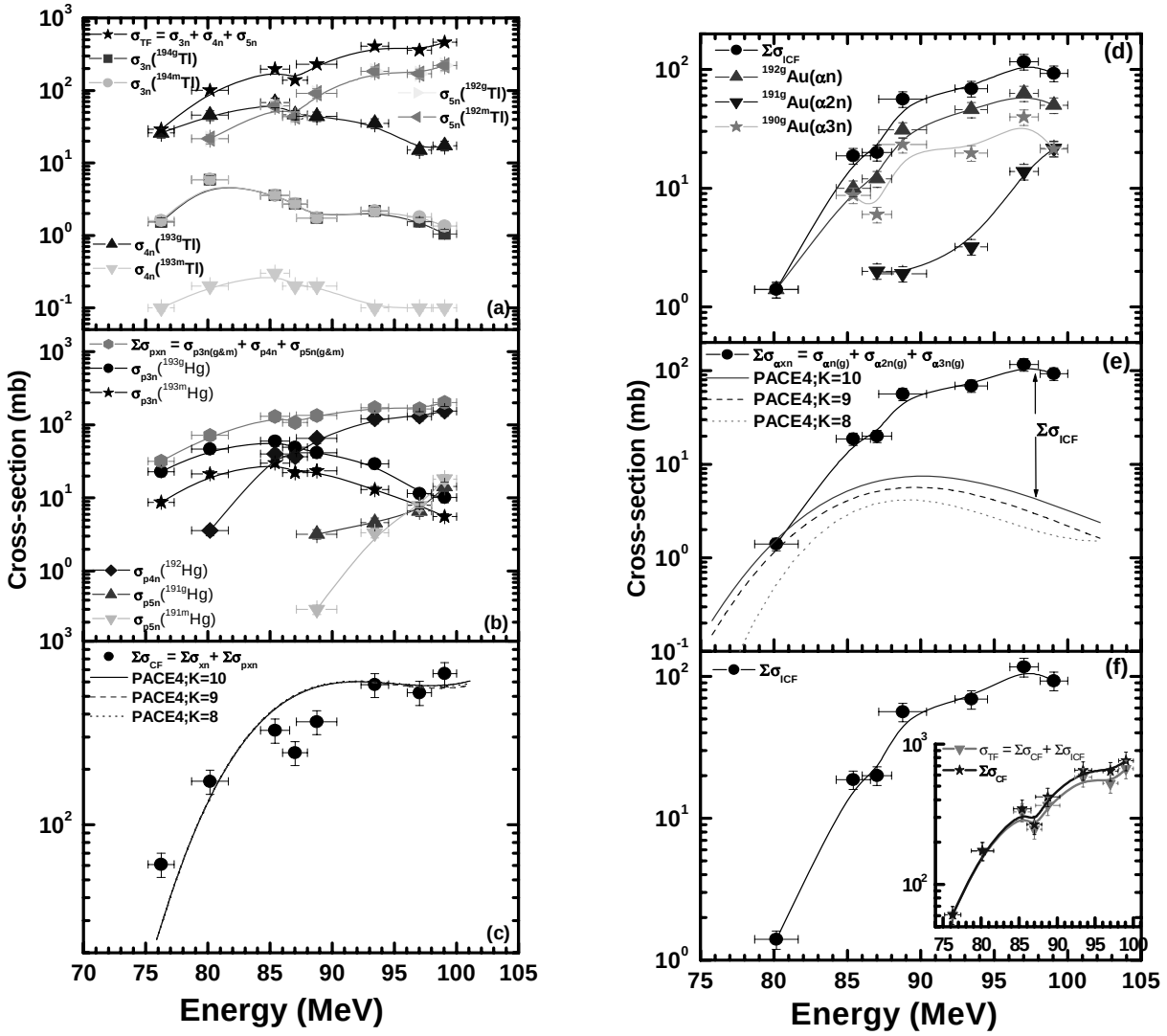

Fig. 2. Experimentally measured cross-sections for various reactions. Lines are drawn to guide the eyes. In Figs. 2(c) & 2(e), theoretical calculations of PACE4 are also shown.

In this case the excited nucleus formed by the fusion of ^{12}C may emit neutrons while de-exciting. Option (i) refers to CF and option (ii) ICF. In Fig.2(d) the sum of cross-sections for all measured αxn channels i.e., $\Sigma\sigma_{\alpha xn}$(expt) is also shown and is found to increase with energy. It has already been mentioned that all the α-emission channels identified in the present work are expected to have significant contribution from ICF processes. In order to determine the contribution from ICF processes to the αxn channels, the measured $\Sigma\sigma_{\alpha xn}$(expt) has been compared with the corresponding values calculated using the theoretical model code PACE4. Since, the code does not take ICF into consideration, the calculated cross-sections for $\Sigma\sigma_{\alpha xn}$ with code PACE4 will have predictions based on CF model only. In Fig.2(e) a comparison of $\Sigma\sigma_{\alpha xn}$(expt) has been made with $\Sigma\sigma_{\alpha xn}$(Th) calculated theoretically using CF model, for three different values of physically acceptable[24] level density parameters (K=8, 9, &10). As can be seen from this figure, the

$\Sigma\sigma_{\alpha xn}$(Th), with any of the reasonable parameters could not reproduce $\Sigma\sigma_{\alpha xn}$(expt) above 85 MeV. The measured $\Sigma\sigma_{\alpha xn}$(expt) agree very well with $\Sigma\sigma_{\alpha xn}$(Th) at 80 MeV. However, above this data point all the measured cross-sections are found to be much higher as compared to that of theoretical pridictions based on PACE4 model. The difference between the experimental and the theoretical values of $\Sigma\sigma_{\alpha xn}$ may be assigned to ICF and is denoted by $\Sigma\sigma_{ICF}$ (expt). Further, the difference between $\Sigma\sigma_{\alpha xn}$(expt) and $\Sigma\sigma_{\alpha xn}$(Th) is found to increase with energy above 80 MeV, indicating the dominance of ICF processes at relatively higher energies, with maximum ICF contribution at highest studied energy i.e., 100 MeV. Further, in Fig.2(f) $\Sigma\sigma_{ICF}$ obtained by subtracting $\Sigma\sigma_{ICF}$ (Th) (K=10) from measured $\Sigma\sigma_{\alpha xn}$ has been plotted as a function of energy. As can be seen from this figure that ICF production increases very rapidly with energy. In the inset of Fig.3(c) $\Sigma\sigma_{TF}$ (total sum of cross-sections for all measured channels) and $\Sigma\sigma_{CF}$ are compared. As can be seen from Fig.2(f) (inset), with the increase in energy the difference between σ_{TF} and $\Sigma\sigma_{CF}$ goes on increasing, indicating the dominance of ICF at relatively higher energies.

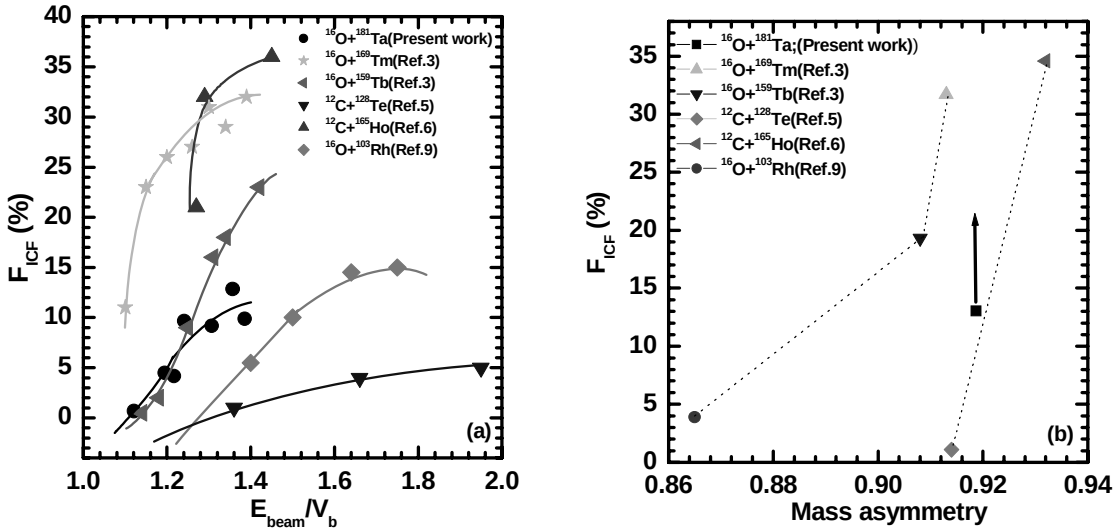

Fig. 3: (a) Deduced percentage ICF fraction (F_{ICF}) as a function of normalised projectile energy alongwith literature values and (b) The percentage F_{ICF} as a function of mass asymmetry at a constant normalized projectile energy.

Further, in order to study the dependence of ICF contribution on energy, for the presently studied system, the percentage fraction of ICF fusion cross-section (FICF) has been plotted in Fig. 3(a), as a function of beam energy normalized to CB, alongwith the several other literature values[3, 5, 6, 9]. As can be seen from this figure FICF increases with the increase in normalized beam energy for all the systems. In order to study the dependence of FICF on mass asymmetry, the $\%F_{ICF}$ has also been plotted as a function of mass asymmetry at a constant value (E_{beam}/V_b=1.38) of normalized beam energy in Fig. 3(b). As can be seen from this figure, the FICF for the presently studied system is not following the expected trend shown for other systems involving ^{16}O beam. The present FICF for ^{16}O+^{181}Ta, is found to be significantly small. It may be because of the fact that in the present measurements several other α-emission channels e.g., (2αxn and 3αxn channels) could not be observed as the residues populated via these channels are either

stable or are short lived and/or having very low γ-rays intensity. We propose to measure the contribution of these α-emission channels in an in-beam experiment using particle-gamma co-incidence technique, so that the present data may be supplemented.

In the present work, EFs for the production of 14 radio nuclides ^{194g}Tl(3n), ^{194m}Tl(3n), ^{193g}Tl(4n), ^{193m}Tl(4n), ^{192g}Tl(5n), ^{192m}Tl(5n), ^{193g}Hg(p3n), ^{193m}Hg(p3n), ^{192}Hg(p4n), ^{191g}Hg(p5n), ^{191m}Hg(p5n), ^{192g}Au(αn), ^{191g}Au(α2n) and ^{190g}Au(α3n) have been measured. The experimental data have been compared with the predictions of theoretical code PACE4 based on statistical model. The CF cross-sections are found agree with PACE4 calculations over the entire energy range. A significant enhancement in the cross-sections has been observed, for α-emitting channels, as compared to the theoretical PACE4 model predictions. The observed enhancement has been attributed to the prompt break-up of the projectile in to α-clusters; (^{16}O into ^{12}C+^{4}He) leading to the ICF process. As such, it may be concluded that apart from CF, the ICF is also a process of greater importance even at these low energies and hence, while predicting the total reaction cross-sections, ICF contribution should also be taken into consideration. Further, as expected $\Sigma\sigma_{ICF}$ is found to increase with energy.

Acknowledgments

The authors are thankful to Prof. Amit Roy, Director, Inter-University Accelerator Centre (IUAC), New Delhi, INDIA for extending all the necessary facilities for performing the experiments and hospitality. We are also thankful to Dr. R. K. Bhaumik, for scientific discussions and supports during the experiments. One of the authors RP thanks to the DST and UGC. Authors also thank the Chairman, Department of Physics, Aligarh Muslim University, Aligarh for providing all the necessary facilities.

References

[1] M. Cavinato, E. Fabrici, E. Gadioli, E. Gadioli Erba, P. Vergani, M. Crippa, G. Colombo, L . Redaelli, and M. Ripamonti, Phys. Rev. C 52, 2577 (1995).
[2] E. Gadioli, C. Brattari, M. Cavinato, E. Fabrici, E.Gadioli Erba, V. Allori, A. Di. Fillippo, S. Vailati, T.G. Stevens, S. H. Connell, J. P. F. Sellschop, F. M.Nortier, G. F. Steyn, C. Marchetta; Nucl. Phys. A641,271 (1998).
[3] Pushpendra P. Singh, B. P. Singh, Manoj Kumar Sharma, Unnati, Devendra P. Singh, Rakesh Kumar, K.S. Golda and R. Prasad, Phys. Rev. C 77, 014607 (2008).
[4] Pushpendra P. Singh, Manoj Kumar Sharma, Unnati, Devendra P. Singh, Rakesh Kumar, K.S. Golda, B. P.Singh and R. Prasad, Eur. Phys. J. A 34, 29 (2007).
[5] Manoj Kumar Sharma, B. P. Singh, Sunita Gupta, M.M. Muthafa, H. D. Bhardwaj and R. Prasad, Journal of Physical Society of Japan 72, 1917 (2003).
[6] Sunita Gupta, B. P. Singh, M. M. Musthafa, H. D.Bhardwaj and R. Prasad; Phys. Rev. C 61, 064613(2000).
[7] M. Blann, Ann. Nucl. Sci. 25, 123 (1975).
[8] Manoj Kumar Sharma, Unnati, B. P. Singh, Rakesh Kumar, K. S. Golda, H. D. Bhardwaj and R. Prasad; Nucl. Phys. A 776, 83 (2006).

[9] Unnati, Pushpendra P. Singh, Devendra P. Singh, Manoj Kumar Sharma, Abhishek Yadav, Rakesh Kumar, B. P.Singh, and R. Prasad; Nucl. Phys. A 811, 77 (2008).
[10] Pushpendra P. Singh, B. P. Singh, Manoj Kumar Sharma, Unnati, Rakesh Kumar, K. S. Golda, D. Singh,R. P. Singh, S. Muralithar, M. A. Ansari, R. Prasad and R. K. Bhowmik; Phys. Rev. C 78, 017602 (2008).
[11] S. M. Mullins; Phys. Rev. C 61, 044315 (2000).
[12] G. J. Lane, G. D. Dracoulis, A. P. Byme, T. R. McGoramand A. R. Poletti; American Institute of Physics, Conference proceeding, 481, 304 (1999).
[13] T. Udagawa et al., Phys. Rev. Lett. 45, 1311 (1980).
[14] J. Wilczynski et al., Phys. Rev. Lett. 45, 606 (1980).
[15] J.P. Bondrof et al., Nucl. Phys. A333, 285(1980).
[16] M. Blan et al., Phys. Rev. Lett.45, 337(1971).
[17] R. Weiner et al., Nucl. Phys. A 286, 282 (1977).
[18] V. I. Zagrebaev; Ann. Phys. (N. Y.)197, 33(1990).
[19] B. G. Harvey; Nucl. Phys. A444, 498(1985).
[20] H. Mogenstern, W. Bohne, W. Galster, K. Grabisch; Z.Phys. A324, 443(1986).
[21] E. Browne and R.B. Firestone, Table of Radioactive Isotopes(Wiley, New York, 1986).
[22] U. Reus, W. Westmeirer, Atomic Data and Nuclear DataTables 29, 338(1983).
[23] A. Gavron, Phys. Rev.C 21, 230 (1980).
[24] M. Blann, G. Reffo, F. Fabbri; Nucl. Instrum. Methods A 265, 490(1988).